An Auto-regressive Model for an Arterial Continuous Glucose Monitoring Sensor

Tony Zhou*, Jennifer Dickson*, J. Geoffrey Chase *

** Department of Mechanical Engineering, University of Canterbury, Christchurch, New Zealand (e-mail: tony.zhou@canterbury.ac.nz).*

Abstract: Continuous glucose monitoring (CGM) devices have the potential to reduce nurse workload in the ICU while improving glycaemic control (GC). However, larger point accuracy errors that are inherent in these devices can lead to adverse consequences for GC performance and safety. There is a need to characterize this error, caused by drift and sensor noise, to evaluate the impact it would have on GC when using CGM devices instead of intermittent blood glucose (BG) measurements. This paper presents an auto-regressive model to model the drift and sensor noise, which can then be used to simulate further CGM sensor traces. Validation by comparison between the original clinical data and the simulated sensor data is used to provide qualitative and quantitative assurance of model accuracy. The auto-regressive model and simulated CGM sensor traces are found to represent the Glysure CGM sensor well, and capture all necessary sensor behaviors.

Keywords: Critical care, disease control, identification and validation, healthcare management, time series modelling

1. INTRODUCTION

Critically ill patients commonly experience insulin resistance and stress induced hyperglycaemia (Capes et al., 2000; Krinsley, 2003; van den Berghe et al., 2001), which has been associated with increased morbidity and mortality (Capes et al., 2000; Krinsley, 2003; Umpierrez et al., 2002). Some studies have shown glycaemic control (GC) can reduce hyperglycaemia and improve outcomes (Chase et al., 2008b; Krinsley, 2004; van den Berghe et al., 2001). However, other studies have failed to replicate these results (Brunkhorst et al., 2008; Finfer et al., 2009; Hirasawa et al., 2009), with some even reporting an increase in mortality (Finfer et al., 2009).

A potential confounding factor is the increased hypoglycaemia observed across almost all these studies (Wiener et al., 2008). Hypoglycaemia is associated with increased mortality (Bagshaw et al., 2009; Egi et al., 2010; Finfer et al., 2012), with one study showing increased mortality after a single event (Bagshaw et al., 2009). Thus, it is important that GC protocols are able to treat hyperglycaemia safely and effectively to achieve the potential outcome benefits.

Hypoglycaemia often occurs where infrequent blood glucose (BG) measurements combine with changes in patient response to care (Chase et al., 2008a; Chase et al., 2006). Continuous glucose monitoring (CGM) devices could help provide safety from hypoglycaemia, reduce workload by increasing automation, and improve GC. The increased temporal resolution CGM devices provide can monitor real-time BG trends, allowing more rapid response to changes to avoid hypoglycaemia.

CGM devices can also reduce GC related nursing workload, providing more data with lower blood sampling requirements (Boom et al., 2014; Holzinger et al., 2010; Signal et al., 2010). However, the increased temporal measurement resolution CGM devices provide is still somewhat outweighed by the larger errors in these devices due to sensor drift, bias, and noise (Facchinetti et al., 2014; Kuure-Kinsey et al., 2006; Reifman et al., 2007; Signal et al., 2010; Zimmermann et al., 2012). There is thus a need to model and account for sensor error when integrating CGM sensors in GC.

The Glysure (GlySure Limited, UK) sensor is a CGM device that measures venous BG via an intravenous line. This paper presents an auto-regressive (AR) method and model characterising the Glysure CGM sensor. This model is compared to clinical data to assess validity, and the overall modelling method is generalisable.

2. METHOD

2.1 Sensor Modelling

2.1.1 Clinical Data

Data from a pilot trial of the Glysure CGM device on 33 cardiac intensive care patients for an average of 37.6 hours is used. It was an observational trial and CGM measures were not used for GC. The sensor provides a new reading 4 times per minute. Intermittent BG measures are used to calibrate the sensor approximately every 8 hours. Intermittent BG measures not used to calibrate the sensor were taken approximately every 2.5 hours. Data from 2 patients was discarded due to sensor failure.

2.1.2 Sensor Characterisation

Sensor characterisation two auto-regressive (AR) models to capture drift and higher frequency sensor fluctuations. Drift is

characterised as the percentage difference between sensor and reference measurements. It is assessed half-hourly using BG interpolated from the calibration and reference measurements. Half hourly interpolation of intermittent BG measures is defined:

$$BG_{IM/30\,min} = interp(BG_{IM})|_{t=0:30:t_{end}} \quad (1)$$

Half hourly sampling of the CGM sensor trace is defined:

$$BG_{SG/30\,min} = sample(BG_{sensor})|_{t=0:30:t_{end}} \quad (2)$$

The percentage drift is calculated from these values such that:

$$Drift = \frac{BG_{SG/30\,min} - BG_{IM/30\,min}}{BG_{IM/30\,min}} \quad (3)$$

A lag-2 AR model was the used to characterise drift, defined:

$$Drift_{n+1} = \alpha_d + \beta_d * Drift_{n-1} + \gamma_d * Drift_n + \xi_d \quad (4)$$

Model parameters α_d, β_d and γ_d are found using linear least squares from half hourly [$Drift_{n+1}$, $Drift_n$, and $Drift_{n-1}$] data points derived from the entire clinical data cohort and Equations 1-3, assuming $\xi_d = 0$. The half hourly interpolation interval was chosen to match observed time frames for fluctuations in BG across the sensor clinical data.

Having identified a best fit α_d, β_d and γ_d, a noise term was calculated by re-arranging Equation 4 and solving for the residuals, ξ_d. Outlier drifts from Equation 3 of more than ±25%, the threshold capturing over 99.3% of the data, were discarded to maintain sufficient data density for probability modelling. The results are used to create a drift noise model by smoothing a continuous distribution function across ξ_d residual results using Equation 4 and all the data.

Sensor noise fluctuations is assessed every 0.25 minutes and sampled from the interpolated BG and CGM device measurements such that:

$$BG_{base/0.25\,minutes} = interp(BG_{SG/30min})|_{t=0:0.25:t_{end}} \quad (5)$$

The fractional difference between these linearly interpolated 'base' BG points and the real sensor trace is defined:

$$SensorFlux = \frac{BG_{sensor} - BG_{base/0.25\,minutes}}{BG_{base/0.25\,minutes}} \quad (6)$$

Another lag-2 AR model is used to characterise these high frequency sensor fluctuations such that:

$$SensorFlux_{n+1} = \alpha_{sf} + \beta_{sf} * SensorFlux_{n-1} + \gamma_{sf} * SensorFlux_n + \xi_{sf} \quad (7)$$

The model parameters α_{sf}, β_{sf} and γ_{sf} are found using the entire data cohort and linear least squares from 0.25 minute [$SensorFlux_{n+1}$, $SensorFlux_n$, and $SensorFlux_{n-1}$] data points derived from clinical data and Equation 6, assuming $\xi_{sf} = 0$.

After identifying a linear best fit for α_{sf}, β_{sf} and γ_{sf} across the entire data cohort, the sensor fluctuation noise term was calculated by re-arranging Equation 7 and solving for the residuals, ξ_{sf}. Outlier fluctuations of more than ±1%, which includes over 99.9% of the data, were discarded. These results are used to create a sensor fluctuation noise model, similar to the drift noise model, by smoothing a continuous distribution function across the data range of ξ_{sf}.

An example of the modelling process is shown using data from Patient 2 in Figure 1. Figure 1a shows the sensor clinical data for Patient 2 over the first 16 hours. Figures 1b and 1c show characterisation of the AR drift model using Equations 3 and 4, where Figure 1c shows the plane of best fit for model parameters α_d, β_d and γ_d, and the drift noise term definition (ξ_d). Figures 1d-1f show characterisation of the sensor fluctuation model using Equation 6 and 7, with planes of best fit for model parameters α_{sf}, β_{sf} and γ_{sf} and the sensor fluctuations noise term definition (ξ_{sf}).

2.2 Sensor Simulation

Sensor simulation is where a sensor trace is simulated from intermittent BG measures. Intermittent BG measures are used as a base to simulate the CGM sensor. They are interpolated half hourly, and drift applied using Equation 4. The resulting BG with drift is:

$$BG_{base(t=0:30:t_{end})} = BG_{IM/30\,minutes}(1 + Drift) \quad (8)$$

Where *Drift* is calculated using Equation 4, with ξ_d drawn randomly from the cohort probability distribution generated from the clinical data. At t = 0, and at any calibration BG, the condition [$Drift_n$, $Drift_{n-1}$] = [0.0, 0.0] is used to recalibrate the CGM sensor to match the simulated intermittent BG measurement, similar to the actual sensor process.

The simulated sensor output is then defined:

$$BG_{new\_sensor(t=0:0.25:t_{end})} = BG_{base/0.25\,minutes}(1 + SensorFlux) \quad (9)$$

Where *SensorFlux* is calculated according to Equation 7, with ξ_{sf} drawn randomly from the cohort probability distribution generated from clinical data. $BG_{base/0.25\,minutes}$ is now:

$$BG_{base/0.25\,minutes} = interp(BG_{base})|_{t=0:0.25:t_{end}} \quad (10)$$

Once again, at t = 0 and any calibration BG, the condition [$SensorFlux_n$, $SensorFlux_{n-1}$] = [0.0, 0.0] is used to recalibrate the CGM sensor. An additional limit of a maximum drift of 40% was applied to the drift AR model matching extremes seen in the clinical sensor data.

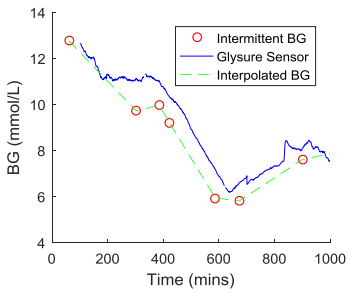

a) Clinical data plotted for Patient 2.

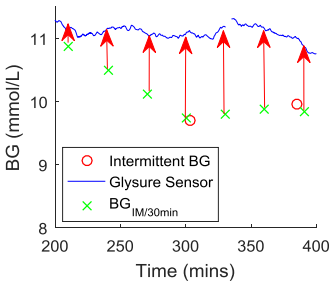

b) Patient 2 with BG resampled every half hour. Red arrows show how *Drift* was characterised (*Drift* = ($BG_{SG/30min}$-$BG_{IM/30min}$)/$BG_{IM/30min}$)

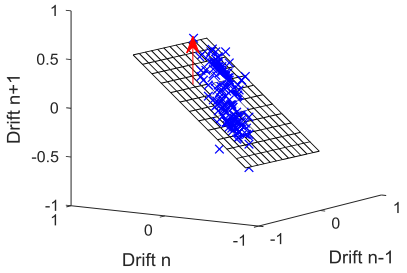

c) $Drift_{n+1}$ plotted against current ($Drift_n$) and previous ($Drift_{n-1}$) for all patients. The plane of best fit is shown in black, with a red arrow showing how ξ_d is sampled.

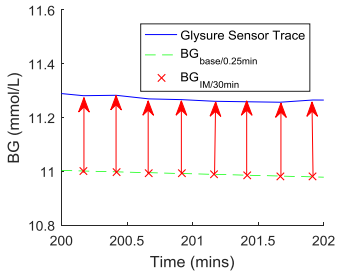

d) Patient 2 with BG resampled every minute. Red arrows show how the sensor fluctuation was characterised.

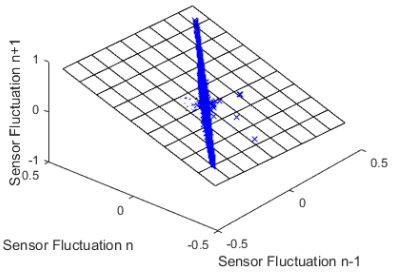

e) $SensorFlux_{n+1}$ plotted against $SensorFlux_n$ and $SensorFlux_{n-1}$ for all patients. The plane of best fit is shown.

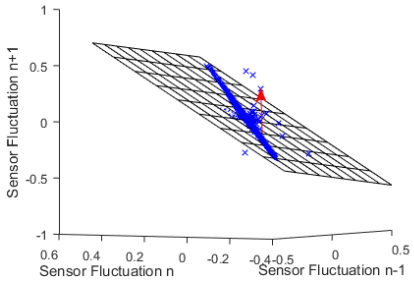

f) $SensorFlux_{n+1}$ plotted against $SensorFlux_n$ and $SensorFlux_{n-1}$ with a red arrow showing how the ξ_{sf} is sampled for the fluctuations.

Figure 1. Steps of the sensor characterisation process, showing how the drift and sensor fluctuations were characterised.

Setting [$Drift_n$, $Drift_{n-1}$] = [0.0, 0.0] and [$SensorFlux_n$, $SensorFlux_{n-1}$] = [0.0, 0.0] effectively applies a point to point recalibration allowing the sensor trace to go through a recalibration point. Divergence from the interpolated BG is then initiated by the ξ_d and ξ_{sf} terms. Figure 2 outlines the steps that occur during the simulation, with a sensor trace and virtual patient forward simulated for the first 4 hours in Figure 2(a).

2.3 Sensor Model Validation

Sensor traces are simulated using intermittent BG from the clinical data cohort from which the model was built. To test consistency between the model and the sensor clinical data, several sensor simulations were overlaid with the clinical data and compared. If the clinical sensor traces were difficult to visually distinguish from simulation, then the model was qualitatively accepted as broadly capturing key behaviour.

To quantitatively validate the model, a simulation was run to generate a single sensor trace from the sensor model for each patient to compare to the sensor clinical data. The mean absolute relative difference (MARD) distributions for the simulations and the sensor clinical data were compared, and a Clarke Error Grid (CEG) plot and Bland-Altman plot constructed. A CEG plot was used to further validate the sensor model against the clinical data. A Bland-Altman plot enabled analysis of any differences in bias behaviour between actual and modelled sensor traces.

3. RESULTS AND DISCUSSION

3.1 Sensor Characterisation

Table 1 gives sensor model parameters identified from the cohort data, and Figure 3 shows the noise term models for drift and sensor fluctuations, ξ_d and ξ_{sf}. Figure 4 shows an example patient with the real sensor trace plotted alongside simulated traces. Sensor behaviour is visually consistent between simulated and real sensor traces, with drift and sensor fluctuations of approximately the same magnitude across all traces.

Figure 5 shows the MARD distribution over the total clinical and simulated clinical data. The simulated data distribution is slightly tighter than the clinical data at the extremes. However, it is still very similar, reflecting the non-Gaussian distribution of MARD at these extremes, compared to the Gaussian noise distribution used.

Table 1: Auto-regressive (AR) model parameters for drift and sensor fluctuations

AR Pass	Key Characteristic	α	β	γ	ξ median	ξ max (absolute)	R^2
1	Drift	-0.00096	-0.05877	0.9393	-0.0028	0.2439	0.78
2	Sensor Fluctuations	-4.4e-6	-0.224	1.215	-5.415e-06	0.01	0.99

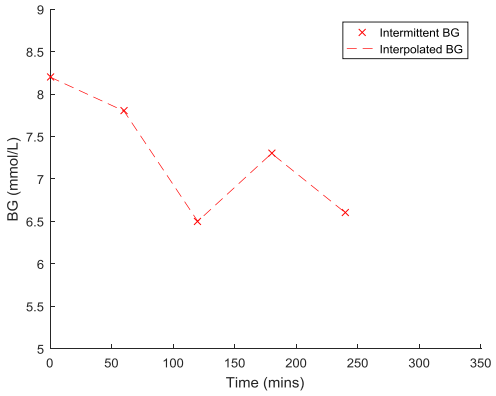

a) An example patient. Intermittent glucometer BG are interpolated between measurements.

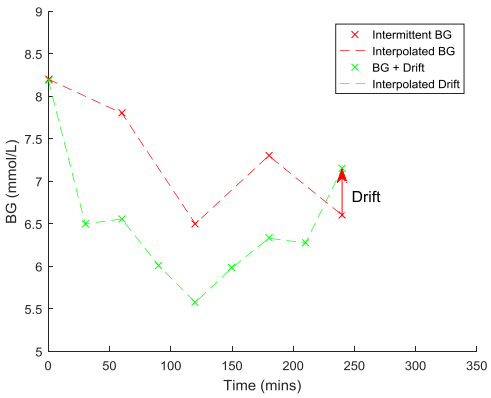

b) AR drift is applied to the interpolated BG at half hour intervals.

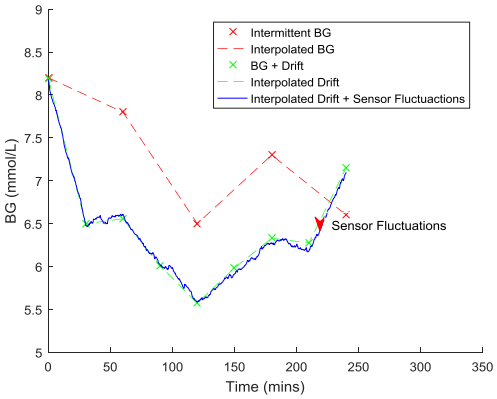

c) AR sensor fluctuations are added to the interpolated AR drift.

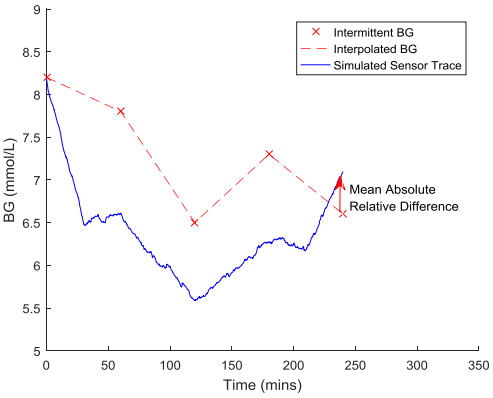

d) Comparison of intermittent BG and final sensor simulation.

Figure 2. Sensor simulation steps during a virtual trial.

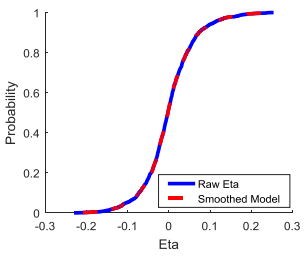

(a) Noise model for drift, ξ_d.

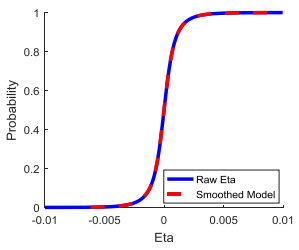

(b) Noise model for sensor fluctuations, ξ_{sf}.

Figure 3: Random noise distributions for auto-regressive drift and sensor fluctuations (fraction)

The Clarke Error Grid (CEG) in Figure 6 shows the model behaves in a consistent manner to the clinical data. At lower BG, where there are fewer data points, error is slightly, though not significantly, overestimated, which is conservative in simulating sensor use in GC. In Figure 7, the Bland-Altman plot shows no significant bias across the observed BG range, and the plotted lines of ±2σ for the clinical and simulated data show the strong similarity between the model outputs and clinical data. Overall, the model is considered to represent the sensor well.

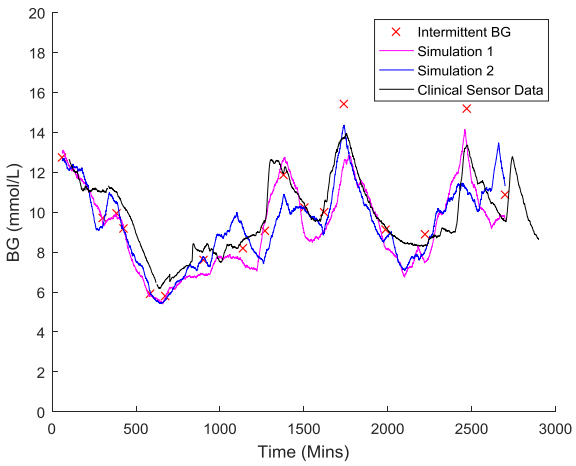

Figure 4. Sensor clinical data with two sensor traces generated from the model.

Worth noting is that the sensor clinical data had almost no BG <5 mmol/L. Underlying sensor model assumptions apply constant sensor behaviour across the full BG range resulting in similar proportional BG error at high and low BG. This assumption is used for lack of other data at this time. In this case, at lower BG, this choice translates to a consistent percentage error, resulting in lower absolute BG errors.

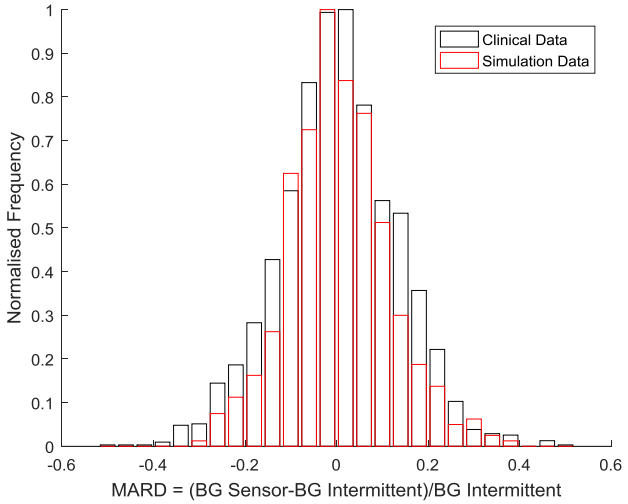

Figure 5. MARD plot of the sensor clinical data vs. the simulated data.

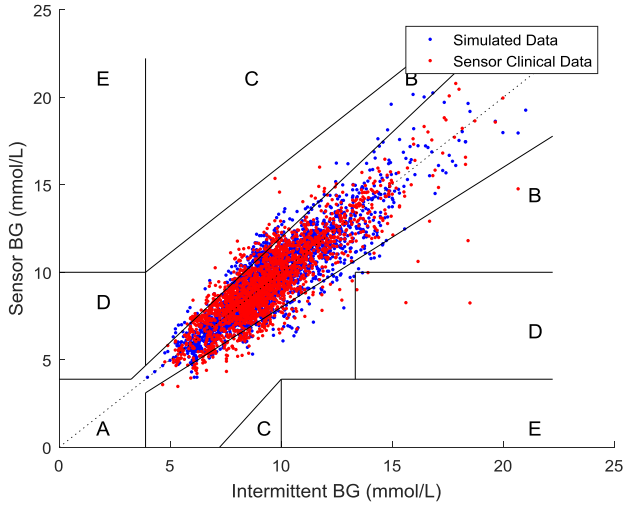

Figure 6. Clarke Error Grid plot of the sensor clinical data and the clinical simulated data, both resampled half hourly.

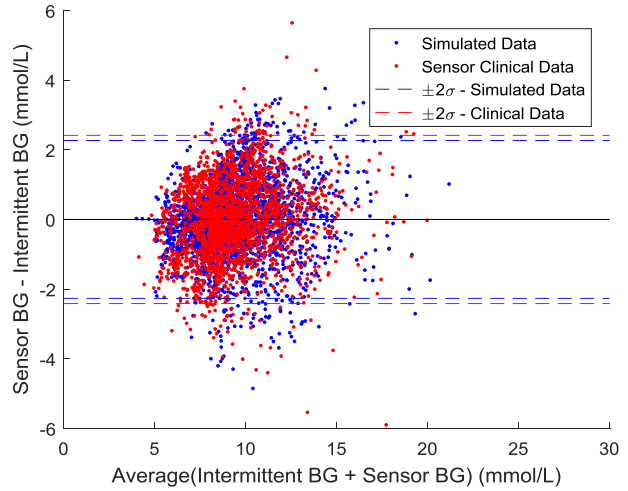

Figure 7. Bland-Altman plot of sensor clinical data and simulated clinical data.

Overall, a sensor model was characterised from clinical data and was found to simulate sensor behaviour well. The MARD distribution and CEG plots for the simulated sensor and the clinical data are very similar. Equally, simulated sensor traces were difficult to visually distinguish from clinical data.

3.2 Limitations

One of the limitations of this study was that in the making of the sensor model, the clinical data used to construct the model had a very low number of BG measurements less than 5 mmol/L. This limitation makes it hard to predict sensor behaviour at this lower BG region, and it was assumed that the sensor behaviour was constant for the range of BG measured. Future research would need to target this region of BG to develop more a reliable sensor model at lower BG.

Another limitation arises from the sensor clinical data, in which there were only 1277 hours of recorded data and the median recording period was 37.6 hours. More data needs to be gathered from patients that stay for longer than 37.6 hours to more accurately model long term sensor measurements in critical care patients.

Finally, the analysis was limited by the amount of patient data from the clinical trial. A larger clinical cohort would have allowed more in-depth analysis through cross-validation. However, the results from the MARD, CEG plot and Bland-Altman plot indicate that there was enough data to generate a satisfactory model.

4. CONCLUSIONS

A CGM sensor model was developed and was able to successfully model the Glysure CGM device. The drift and sensor fluctuations are characterised from clinical data, and then used to simulate the sensor traces on top of the clinical data. The clinical data and simulated data were quantitatively validated through the MARD, CEG plots and Bland-Altman plots, and thus showed that the simulated sensor represented the Glysure CGM sensor well. The overall approach is fully generalisable to similar sensors.

ACKNOWLEDGEMENTS

Clinical data and sensor information provided by Barry Crane and Nick Barlow from GlySure Limited (Oxfordshire, UK). The authors also acknowledge the support of the EUFP7 and RSNZ Marie Curie IRSES program, the Health Research Council (HRC) of New Zealand, the MedTech CoRE and TEC, and NZ National Science Challenge 7, Science for Technology and Innovation.

REFERENCES

Bagshaw, SM, Bellomo, R, Jacka, MJ, Egi, M, Hart, GK, George, C & Committee, ACM (2009), 'The impact of early hypoglycemia and blood glucose variability on outcome in critical illness', *Crit Care*, vol. 13, no. 3, p. R91.

Boom, DT, Sechterberger, MK, Rijkenberg, S, Kreder, S, Bosman, RJ, Wester, JP, van Stijn, I, DeVries, JH & van der Voort, PH (2014), 'Insulin treatment guided by subcutaneous continuous glucose monitoring compared to frequent point-of-care measurement in critically ill patients: a randomized controlled trial', *Crit Care*, vol. 18, no. 4, p. 453.

Brunkhorst, FM, Engel, C, Bloos, F, Meier-Hellmann, A, Ragaller, M, Weiler, N, Moerer, O, Gruendling, M, Oppert, M, Grond, S, Olthoff, D, Jaschinski, U, John, S, Rossaint, R, Welte, T, Schaefer, M, Kern, P, Kuhnt, E, Kiehntopf, M, Hartog, C, Natanson, C, Loeffler, M, Reinhart, K & German Competence Network, S (2008), 'Intensive insulin therapy and pentastarch resuscitation in severe sepsis', *N Engl J Med*, vol. 358, no. 2, pp. 125-139.

Capes, SE, Hunt, D, Malmberg, K & Gerstein, HC (2000), 'Stress hyperglycaemia and increased risk of death after myocardial infarction in patients with and without diabetes: a systematic overview', *Lancet*, vol. 355, no. 9206, pp. 773-778.

Chase, JG, Andreassen, S, Jensen, K & Shaw, GM (2008a), 'Impact of human factors on clinical protocol performance: a proposed assessment framework and case examples', *J Diabetes Sci Technol*, vol. 2, no. 3, pp. 409-416.

Chase, JG, Shaw, G, Le Compte, A, Lonergan, T, Willacy, M, Wong, XW, Lin, J, Lotz, T, Lee, D & Hann, C (2008b), 'Implementation and evaluation of the SPRINT protocol for tight glycaemic control in critically ill patients: a clinical practice change', *Crit Care*, vol. 12, no. 2, p. R49.

Chase, JG, Shaw, GM, Wong, XW, Lotz, T, Lin, J & Hann, CE (2006), 'Model-based glycaemic control in critical care-A review of the state of the possible', *Biomedical Signal Processing and Control*, vol. 1, no. 1, pp. 3-21.

Egi, M, Bellomo, R, Stachowski, E, French, CJ, Hart, GK, Taori, G, Hegarty, C & Bailey, M (2010), 'Hypoglycemia and outcome in critically ill patients', *Mayo Clin Proc*, vol. 85, no. 3, pp. 217-224.

Facchinetti, A, Del Favero, S, Sparacino, G, Castle, JR, Ward, WK & Cobelli, C (2014), 'Modeling the glucose sensor error', *IEEE Trans Biomed Eng*, vol. 61, no. 3, pp. 620-629.

Finfer, S, Chittock, DR, Su, SY, Blair, D, Foster, D, Dhingra, V, Bellomo, R, Cook, D, Dodek, P, Henderson, WR, Hebert, PC, Heritier, S, Heyland, DK, McArthur, C, McDonald, E, Mitchell, I, Myburgh, JA, Norton, R, Potter, J, Robinson, BG & Ronco, JJ (2009), 'Intensive versus conventional glucose control in critically ill patients', *N Engl J Med*, vol. 360, no. 13, pp. 1283-1297.

Finfer, S, Liu, B, Chittock, DR, Norton, R, Myburgh, JA, McArthur, C, Mitchell, I, Foster, D, Dhingra, V, Henderson, WR, Ronco, JJ, Bellomo, R, Cook, D, McDonald, E, Dodek, P, Hebert, PC, Heyland, DK & Robinson, BG (2012), 'Hypoglycemia and risk of death in critically ill patients', *N Engl J Med*, vol. 367, no. 12, pp. 1108-1118.

Hirasawa, H, Oda, S & Nakamura, M (2009), 'Blood glucose control in patients with severe sepsis and septic shock', *World J Gastroenterol*, vol. 15, no. 33, pp. 4132-4136.

Holzinger, U, Warszawska, J, Kitzberger, R, Wewalka, M, Miehsler, W, Herkner, H & Madl, C (2010), 'Real-time continuous glucose monitoring in critically ill patients: a prospective randomized trial', *Diabetes Care*, vol. 33, no. 3, pp. 467-472.

Krinsley, JS (2003), 'Association between hyperglycemia and increased hospital mortality in a heterogeneous population of critically ill patients', *Mayo Clin Proc*, vol. 78, no. 12, pp. 1471-1478.

Krinsley, JS (2004), 'Effect of an intensive glucose management protocol on the mortality of critically ill adult patients', *Mayo Clin Proc*, vol. 79, no. 8, pp. 992-1000.

Kuure-Kinsey, M, Palerm, CC & Bequette, BW (2006), 'A dual-rate Kalman filter for continuous glucose monitoring', *Conf Proc IEEE Eng Med Biol Soc*, vol. 1, pp. 63-66.

Reifman, J, Rajaraman, S, Gribok, A & Ward, WK (2007), 'Predictive monitoring for improved management of glucose levels', *J Diabetes Sci Technol*, vol. 1, no. 4, pp. 478-486.

Signal, M, Pretty, CG, Chase, JG, Le Compte, A & Shaw, GM (2010), 'Continuous glucose monitors and the burden of tight glycemic control in critical care: can they cure the time cost?', *J Diabetes Sci Technol*, vol. 4, no. 3, pp. 625-635.

Umpierrez, GE, Isaacs, SD, Bazargan, N, You, X, Thaler, LM & Kitabchi, AE (2002), 'Hyperglycemia: an independent marker of in-hospital mortality in patients with undiagnosed diabetes', *J Clin Endocrinol Metab*, vol. 87, no. 3, pp. 978-982.

van den Berghe, G, Wouters, P, Weekers, F, Verwaest, C, Bruyninckx, F, Schetz, M, Vlasselaers, D, Ferdinande, P, Lauwers, P & Bouillon, R (2001), 'Intensive insulin therapy in critically ill patients', *N Engl J Med*, vol. 345, no. 19, pp. 1359-1367.

Wiener, RS, Wiener, DC & Larson, RJ (2008), 'Benefits and risks of tight glucose control in critically ill adults: a meta-analysis', *JAMA*, vol. 300, no. 8, pp. 933-944.

Zimmermann, JB, Lehmann, M, Hofer, S, Husing, J, Alles, C, Werner, J, Stiller, J, Kunnecke, W, Luntz, S, Motsch, J & Weigand, MA (2012), 'Design of a prospective clinical study on the agreement between the Continuous GlucoseMonitor, a novel device for CONTinuous ASSessment of blood GLUcose levels, and the RAPIDLab (R) 1265 blood gas analyser: The CONTASSGLU study', *Bmc Anesthesiology*, vol. 12